Local group modes and the dynamics of intramolecular energy transfer across a heavy atom

Vicente Lopez
Departamento Quimica Fisica y Quimica Cuantica, Universidad Autonoma de Madrid, Cantoblanco, 28049 Madrid, Spain

Victor Fairen
Departamento de Termologia, Facultad de Ciencias, Universidad de Valladolid, Valladolid, Spain and Departamento de Fisica Fundamental, UNED, 28003 Madrid, Spain

Steven M. Lederman and R. A. Marcus
Arthur Amos Noyes Laboratory of Chemical Physics, California Institute of Technology,[a] *Pasadena, California 91125*

(Received 29 August 1985; accepted 11 February 1986)

The dynamics of energy transfer is discussed for a model system in which two ligands are separated by a heavy atom. Numerical and analytical results are given for the case that each ligand is a CC. In the quasiperiodic regime, the dynamics are interpreted using perturbation theory. Local group modes involved in an intramolecular energy localization which can occur in this regime are identified. An approximate separation of the primarily ligand–ligand motions from the primarily ligand–metal–ligand ones occurs in the clearly quasiperiodic regime and also at an energy where the power spectra of the bond coordinates are "grassy." The overall analysis is used to make predictions for systems with larger ligands, when the primarily metal atom–ligand modes are, as above, approximately separable from the primarily intraligand ones.

I. INTRODUCTION

In a previous paper[1] we considered the energy transfer between two ligands attached to a heavy atom M. Classical trajectories were calculated for model system C–C–C–M–C–C–C. While energy transfer occurred at low energies, there was only a restricted energy transfer when the energy of one ligand was high enough that the vibration frequencies in the two ligands were no longer "resonant." More recently, calculations[2] were also reported for a system with more coordinates, including bending motions. For excitation energies of 50 kcal mol^{-1}, the energy transfer was restricted for the potential energy surface used.

In the present paper we treat the motion analytically for the five-atom system C–C–M–C–C. The extent of energy transfer in the quasiperiodic regime is analyzed in terms of the "local group modes"—the anharmonic modes for each ligand—using perturbation theory to calculate the properties of these modes. The perturbation theory is also tested by comparison of semiclassical and quantum eigenvalues of a ligand. At high energies a regime that may be partially chaotic occurs for the five-atom system and is discussed.

Based on the analytical and numerical findings in the present paper it is shown how certain features of the results can be extended to larger systems, provided an approximate separation condition is fulfilled.

II. EXCITATION ENERGY AND ENERGY TRANSFER

In this section the results of numerical trajectory calculations are described for the C–C–M–C–C system, where the bonds are, as before, Morse oscillators coupled by the stretching momenta cross terms and where the masses have been chosen to roughly reproduce the C/Sn mass ratio.[1] These calculations are aimed at exploring the range of behavior found in the previous model. Because of the smaller number of coordinates now, a perturbation analysis is simpler. Nevertheless, the qualitative numerical behavior is similar to that found[1] for the seven-atom chain. In the analysis we focus attention on local group modes of each metal–ligand subsystem, the present system being the simplest example where these group modes can be studied.

The model Hamiltonian used is

$$H=\frac{1}{2}\sum_{i,j=1}^{4} g_{ij}\,p_i\,p_j+\sum_{i=1}^{4} D_i\left[1-e^{-a(r_i-r_i^e)}\right]^2, \quad (1)$$

where the g_{ij}'s are the usual Wilson G-matrix elements[3] that couple adjacent bonds. The Morse potential parameters are the same as those in Ref. 1, namely, $D_i = 84.1$ kcal mol^{-1}, $a = 1.54$ Å^{-1}, and $r_i^e = 1.54$ Å (cf. Ref. 1 for precise values in a.u.). The r_i's in Eq. (1) are the bond distances and the p_i's denote their canonically conjugate momenta. In order to describe the energy transfer across the heavy atom, approximate energies E_L and E_R for both halves of the model chain (the left containing $i = 1,2$ and the right containing $i = 3,4$) are defined in such a way that the Hamiltonian (1) can be rewritten as

$$H = H_L + H_R + V_{LR}, \quad (2)$$

where

$$E_L = H_L = H_1 + H_2 + g_{12}\,p_1\,p_2, \quad (3a)$$

$$E_R = H_R = H_3 + H_4 + g_{34}\,p_3\,p_4, \quad (3b)$$

$$V_{LR} = g_{23}\,p_2\,p_3, \quad (3c)$$

and H_i ($i = 1$–4) denotes the Hamiltonian of the ith Morse bond given by

$$H_i = \tfrac{1}{2}g_{ii}\,p_i^2 + D\left[1-e^{-a(r_i-r_i^e)}\right]^2. \quad (4)$$

Equation (4) can be reduced to its normal form

[a] California Institute of Technology Contribution No. 7255.

 0021-9606/86/105494-10$02.10

$$H_i = J_i\omega_i^0(1-\chi_i J_i) \tag{5}$$

using the usual action-angle variables[4] related to the bond coordinates and momenta according to

$$J_i = \frac{1}{2\chi_i}\left(1-\left[2z_i - z_i^2 - \frac{g_{ii}\,p_i^2}{2D}\right]^{1/2}\right), \tag{6}$$

$$\phi_i = \cos^{-1}\left(\frac{z_i - 1 + (g_{ii}\,p_i^2/2z_iD)}{[1-2z_i+z_i^2+(g_{ii}\,p_i^2/2D)]^{1/2}}\right), \tag{7}$$

Here,

$$\omega_i^0 = [2Da^2g_{ii}]^{1/2}, \quad \chi_i = \omega_i^0/4D,$$
$$z_i = \exp[-a(r_i - r_i^e)]. \tag{8}$$

The trajectories were calculated with an initial excitation energy E_1 of bond 1. All other bonds were taken to have, at time zero, the zero-point energy value with the action variable $J_i = \frac{1}{2}$ (in units of $\hbar = 1$), $r_i = r_i^e$ and $p_i > 0$. A predictor–corrector method[5] with double precision arithmetic was first used to perform the numerical integration of Hamilton's equations of motion. All forward trajectories were back integrated to check their reliability and the initial conditions were found to be preserved for all but one trajectory, discussed later, that at $E_1 = 0.5$ D. To back integrate the latter it was necessary to go to the unusual step of using quadruple precision.[5] All trajectory data given in the present paper are now quadruple precision, with initial conditions being preserved, on back integration, to within 0.01%.

In Fig. 1 the time evolution of E_L and E_R is depicted for an initial excitation of bond 1 to $E_1 = 0.3$ D. When averaged over an ensemble of trajectories with the same initial excitation energy E_1 and different phases for bond 1, the oscillating components in E_L and E_R disappear, while the nonequilibrated final distribution of energy is preserved. There is an excess of energy in the originally excited left-hand side of the molecule. While the excitation is redistributed between the bonds 1 and 2 in less than a picosecond, no complete energy transfer is observed across the heavy atom for a time of integration as long as 0.25 ns for the cited initial energy E_1. (Approximately 25 harmonic oscillations of each C–C bond occur per picosecond.) Results for only a portion of the total trajectory time are given in Fig. 1, the remaining portion being similar to that depicted there.

In Fig. 2 power spectra of the dynamical variable r_1 and its symmetric counterpart r_4 are given for the above trajectory. The spectra show that the motion is regular (quasiperiodic). The coordinates have the same frequencies, as they should in a coupled system, with a different intensity pattern as expected. The four fundamental frequencies should appear in pairs, due to the symmetry of the model chain. The fundamentals occur near $\omega = 3$ and 7 (units in caption).

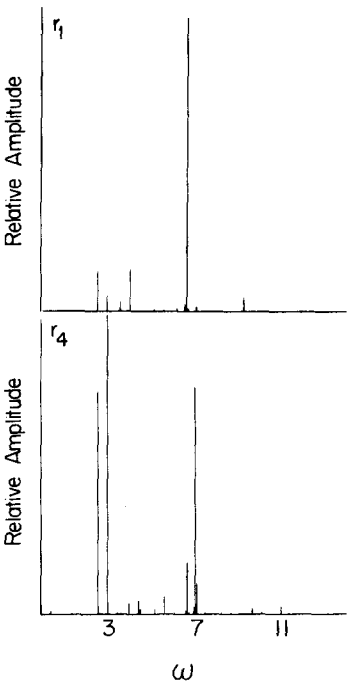

FIG. 2. Power spectra of bond distances r_1 and r_4 for $E_1 = 0.3$ D and $\phi_1 = 0.5$. The unit of the angular frequency ω is the ω_1^0 given by Eq. (8).

The trajectory used for Fig. 1 is characteristic of a group of trajectories we will refer to as "localizing." They are prevalent for initial conditions corresponding to the energy range $E_1 = 0.15$ to 0.40 D (depending on initial phases, however). "Nonlocalizing" trajectories prevail for energies $E_1 < 0.1$ D. In the latter, energy equilibration between the two halves of the model chain is complete on the time scale of a C–C vibration. Power spectra for variables r_1 and r_4 for such trajectories are rather similar to the r_4 power spectrum displayed in Fig. 2.

When the excitation energy exceeds 0.4 D, the behavior is different, although it is difficult to be precise about the energy range in which this new behavior appears. In Fig. 3 the time evolution of E_L is shown after an initial excitation of bond 1 to an energy of 0.5 D. The trajectory is nonlocalizing and its power spectra (Fig. 4) have a number of grassy peaks; the model chain achieves a complete energy equilibra-

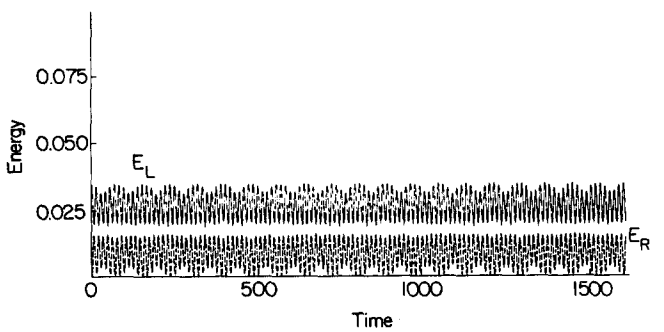

FIG. 1. Energy localization for $E_1 = 0.3$ D and $\phi_1 = 0.5$. Figure depicts E_L and E_R (in a.u.) vs time. (One unit is $2\pi/\omega_1^0$ with ω_1^0 given by Eq. (8) and being about 0.038 ps.)

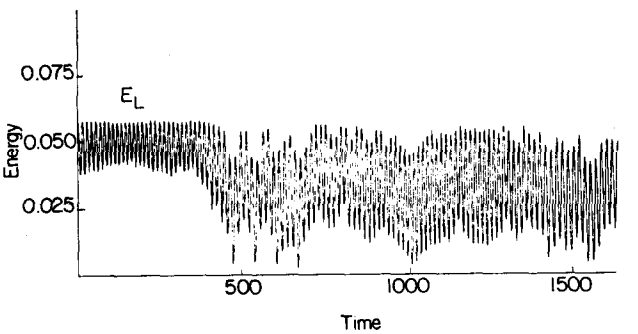

FIG. 3. E_L for a (possibly) chaotic trajectory for $E_1 = 0.5$ D and $\phi_1 = 0.5$ (the same units as in Fig. 2).

tion across the heavy atom after some induction period has elapsed. In the corresponding power spectra for r_1 and r_4 in Fig. 4, a grasslike collection of lines appears that partially replaces the high frequency mode peak found in the previous quasiperiodic trajectories. On the other hand, the two low-frequency mode peaks, red shifted from their values in Fig. 2, still appear to be sharply defined. A combination band at an intermediate frequency has also become grassy.

Finally, at a still higher excitation energy of $E_1 = 0.7$ D, the seeming chaos has disappeared. A typical result is shown in Fig. 5 for the time evolution of E_L and E_R and in Fig. 6 for the power spectra of r_1 and r_4. This result is an example of a localizing trajectory occurring for excitation energies E_1 near D. The intensity pattern in Fig. 6 differs from that in Fig. 1.

The above results summarize the different types of motion and energy transfer that we have encountered in this model system.

III. LOCAL GROUP MODE ANALYSIS

In this section the localization of energy described in Sec. II is analyzed in terms of resonances between the local group modes in each ligand, when the initial excitation of the left ligand is in the moderate energy range, namely for quasiperiodic trajectories in the range $E_1 < 0.4$ D. Local group modes involve a collective motion of the atoms of each ligand. The motion may be compared with that in a symmetric triatomic molecule ABA, with $m_B \gg m_A$. Here, the localization is due to nonlinear resonances between the two local bond modes[6,7] AB and BA. A similar phenomenon is expected to occur in the present symmetric model chain, with a resonance now occurring between corresponding local group modes of each ligand. Only one of the two local group modes in each ligand, it will be shown, actively participates in the localization of energy in the present case.

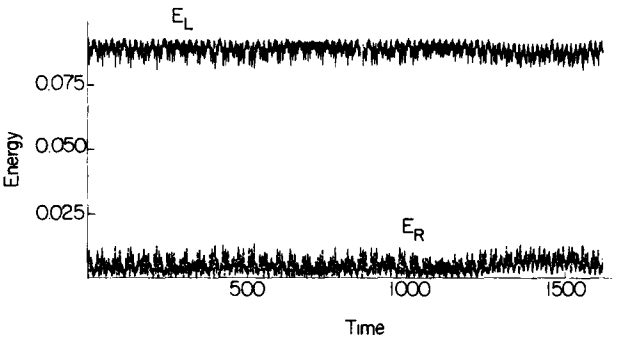

FIG. 5. Energy localization shown in the time evolution of E_L and E_R. $E_1 = 0.7$ D and $\phi_1 = 0.5$ (the same units as in Fig. 1).

The analysis of results in Sec. II is performed by first identifying the local group modes of each ligand–metal subsystem. In the moderate to low energy range in which they occur ($E_1 < 0.4$ D), we will presume they are somewhat perturbed from the harmonic local group modes, i.e., from the standard normal modes of the ligand–metal subsystem. The corrections to normal modes are found in Appendix A using a Birkhoff–Gustavson perturbation scheme. In that analysis the Hamiltonians H_L and H_R in Eq. (3) are each cast into normal form [Eqs. (A11) and (A13)]. They are thereby expressed in terms of a polynomial in the local group mode actions, a polynomial generated here using terms up to and including fourth order analytically and sixth order numerically. The resulting H_L and H_R do not depend upon the new angle variables. The corresponding new action variables are thereby, within this order of approximation, constants of motion for L–M and M–R, respectively. Physically, the two anharmonic local group modes in a ligand represent a primarily C–C stretching motion (termed the "X mode") and a primarily C–C group vs M motion (termed the "Y mode").[8] The Y mode has a lower frequency of oscillation, due to a

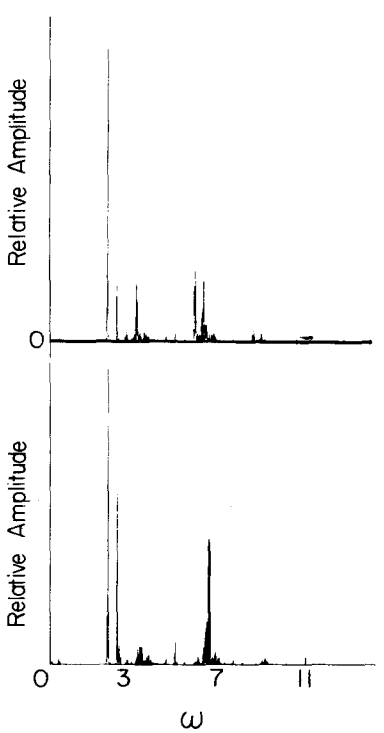

FIG. 4. Power spectra of bond distances r_1 and r_4 for $E_1 = 0.5$ D and $\phi_1 = 0.5$ for the trajectory used for Fig. 3 (the same units as in Fig. 2).

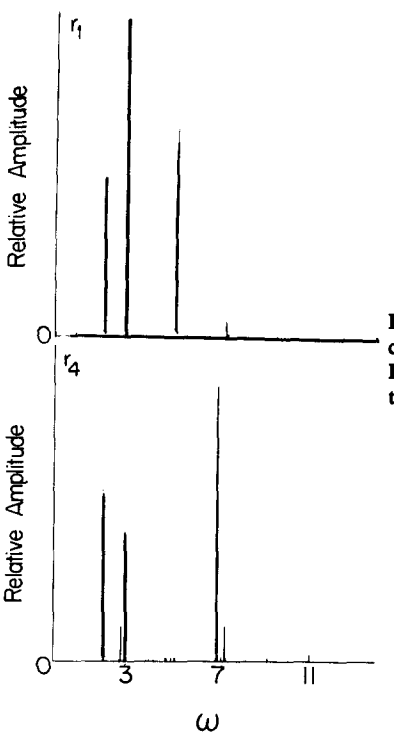

FIG. 6. Power spectra of bond distances r_1 and r_4 for $E_1 = 0.7$ D and $\phi_1 = 0.5$ for the trajectory used for Fig. 5.

higher effective mass. This perturbation scheme also yields the generating function needed to transform the original to the new action-angle variables.

Once an approximation to H_L and H_R has been constructed in terms of the actions of the local group modes, these expressions are introduced into Eq. (2), while the complicated expression for V_{LR} in terms of action-angle coordinates is expressed in terms of a Fourier series in the angle coordinates φ_x and φ_y for the X and Y modes for the left ligand and $\varphi_{x'}$ and $\varphi_{y'}$ for the equivalent X' and Y' modes for the right ligand. The resulting equation is

$$H = \sum_{n=1}^{\infty} \sum_{i+j=n} C_{ij} (J_x^i J_y^j + J_{x'}^i J_{y'}^j) + \sum_{k,l,n,m} V_{klmn} (J_x, J_{x'}, J_y, J_{y'}) \times \exp[i(k\varphi_x + l\varphi_y + m\varphi_{x'} + n\varphi_{y'})]. \quad (9)$$

In the standard Chirikov analysis[9,10] of nonlinear resonances, only the leading terms of the expansion are usually taken into account. In the present problem we make the same approximation and see how well the results serve to interpret the trajectory results. From Eq. (A11) and leading terms of the Fourier expansion of V_{LR}, the resulting resonance Hamiltonian is[11]

$$H = \omega_{0x}(J_x + J_{x'}) + \omega_{0y}(J_y + J_{y'}) - \lambda_x (J_x^2 + J_{x'}^2) - \lambda_y (J_y^2 + J_{y'}^2) - \lambda_{xy}(J_x J_y + J_{x'} J_{y'}) - \epsilon_x (J_x J_{x'})^{1/2} \cos(\varphi_x - \varphi_{x'}) - \epsilon_y (J_y J_{y'})^{1/2} \cos(\varphi_y - \varphi_{y'}). \quad (10)$$

where the λ's are given in Eq. (A12) in Appendix A and the ϵ's in Ref. 11. One omits thereby terms such as $\cos 2(\varphi_x - \varphi_{x'})$ and crossterms such as $\cos(\varphi_x - \varphi_{x'})\cos(\varphi_y - \varphi_{y'})$. However, the omission does not decouple the (X,X') modes from the (Y,Y') ones, since there remain in Eq. (10) the λ_{xy} crossterms.

New variables are next introduced via a canonical transformation

$$\begin{aligned} I_x &= J_x + J_{x'}, & \theta_x &= (\varphi_x + \varphi_{x'})/2, \\ \bar{I}_x &= J_x - J_{x'}, & \bar{\theta}_x &= (\varphi_x - \varphi_{x'})/2, \\ I_y &= J_y + J_{y'}, & \theta_y &= (\varphi_y + \varphi_{y'})/2, \\ \bar{I}_y &= J_y - J_{y'}, & \bar{\theta}_y &= (\varphi_y - \varphi_{y'})/2. \end{aligned} \quad (11)$$

The new action variables $\bar{I}_x$ and $\bar{I}_y$ are particularly suited for monitoring the extent of energy transfer across the heavy atom. They describe what we shall call the $\bar{X}$ and $\bar{Y}$ motion of the molecular system. Equation (10) becomes

$$2H = 2\omega_{0x} I_x + 2\omega_{0y} I_y - \lambda_x (I_x^2 + \bar{I}_x^2) - \lambda_y (I_y^2 + \bar{I}_y^2) - \lambda_{xy}(I_x I_y + \bar{I}_x \bar{I}_y) - \epsilon_x (I_x^2 - \bar{I}_x^2)^{1/2} \cos 2\bar{\theta}_x - \epsilon_y (I_y^2 - \bar{I}_y^2)^{1/2} \cos 2\bar{\theta}_y. \quad (12)$$

As seen from the Hamiltonian in Eq. (12), I_x and I_y are constants of motion in this approximation. Including all the constants in a single term H_c, Eq. (12) may be rewritten as

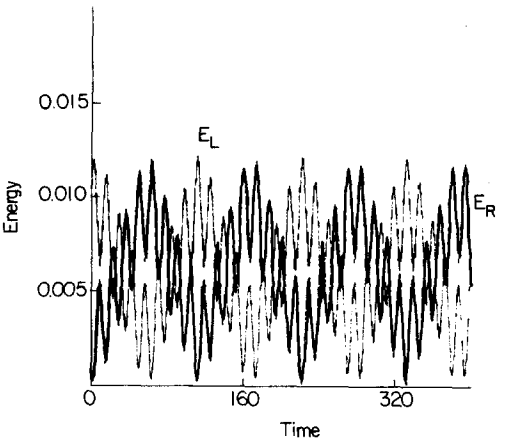

FIG. 7. Time evolution of E_L and E_R for nonlocalizing trajectory. $E_1 = 0.1$ D, $\phi_1 = 0.5$.

$$2(H_c - E) = \lambda_x \bar{I}_x^2 + \lambda_y \bar{I}_y^2 + \lambda_{xy} \bar{I}_x \bar{I}_y + \epsilon_x (I_x^2 - \bar{I}_x^2)^{1/2} \cos 2\bar{\theta}_x + \epsilon_y (I_y^2 - \bar{I}_y^2)^{1/2} \cos 2\bar{\theta}_y. \quad (13)$$

The resulting Hamiltonian is equivalent to that of two coupled hindered rotors, each having a potential which is dependent on the action variables. Their momenta $\bar{I}_x$ and $\bar{I}_y$ represent differences between left and right local group mode actions, as in Eq. (11).

Numerical calculations for the energy and the actions are given in Figs. 7–14. They are made using the trajectory data for the conditions in Figs. 7 and 10 and using the sixth order actions (Appendix A) and the transformation equation (11). The time evolution of E_L and of E_R is depicted in Fig. 7 for a nonlocalizing group mode trajectory, and I_x and I_y for this trajectory are plotted vs time in Fig. 8. It is clear that both I_x and I_y are, as previously suggested, approximate constants of motion. On the other hand, it can be seen in Figs. 9 and 10 that both $\bar{I}_x$ and $\bar{I}_y$ each undergo a change of sign, i.e., they undergo an oscillatory motion. For the localizing trajectory whose energy in each ligand is plotted in

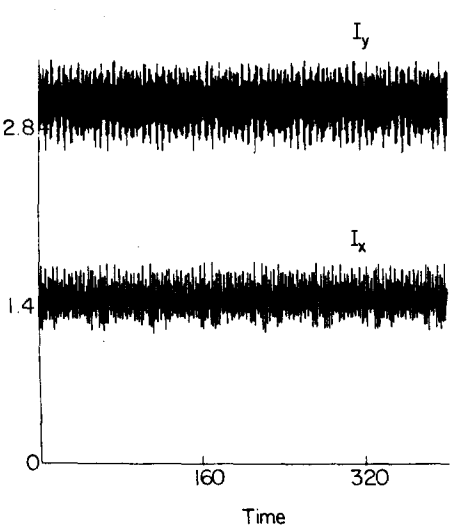

FIG. 8. Approximate invariants of the motion for the I_x and I_y (sixth order) modes of the molecule, corresponding to the trajectory used for Fig. 7.

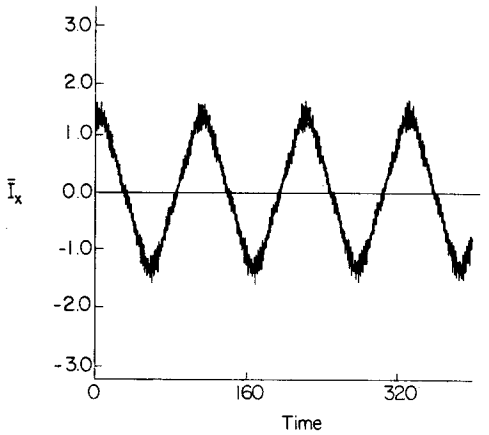

FIG. 9. Oscillating regime near the resonance for $\bar{I}_x$ for the trajectory of Fig. 7.

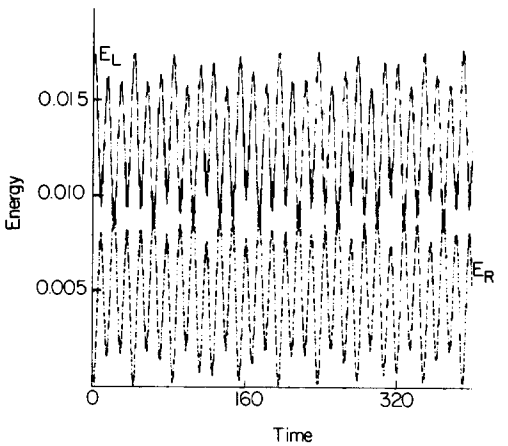

FIG. 11. Time evolution of E_L and E_R for a localizing trajectory. $E_1 = 0.15$ D, $\phi_1 = 0.5$.

Fig. 11, I_x and I_y are again approximate constants of motion (Fig. 12), $\bar{I}_y$ still oscillates (Fig. 13), but the motion of $\bar{I}_x$ has become "rotational", i.e., it no longer changes sign during the motion (Fig. 14). As a consequence there is no longer a complete equilibration of energy between the two ligands. That is, the $\bar{X}$ motion (primarily an antisymmetric ligand–ligand motion) is responsible for the energy localization.

The above results and the behavior of the apparently only partially grassy spectrum in Fig. 4 indicate that the $\bar{X}$ and $\bar{Y}$ motions behave rather independently. They also indicate that although the $\bar{Y}$ motion is only oscillatory in the examples given, the $\bar{X}$ motion has two accessible possibilities, oscillation and rotation. A detailed understanding of this behavior is based on the following analysis.

When the frequency of the $\bar{I}_y$ motion is significantly faster than that for $\bar{I}_x$ as it is in Figs. 9 and 10 and Figs. 13 and 14, the λ_{xy} term tends to average to zero during the slow $\bar{I}_x$ motion. Indeed, a subsequent numerical solution of the equations of motion based on the Hamiltonian (13) showed, for the conditions in Figs. 9 and 10, relatively little effect of the coupling term $\lambda_{xy}\bar{I}_x\bar{I}_y$. It produces the slow modulation of the amplitude of the $\bar{I}_y$ motion noticeable in Fig. 10 and, to a lesser extent, in Fig. 14. For the solution based on Eq. (13), this modulation disappeared when λ_{xy} was set equal to zero. In what follows, we shall assume the $\bar{I}_x$ and $\bar{I}_y$ motions to be largely decoupled by neglecting this λ_{xy} term. However, when the frequencies of those motions become comparable that term should be considered.

With the neglect of λ_{xy}, we may define an "energy" E_α, where α refers to X or Y:

$$2E_\alpha = \lambda_\alpha \bar{I}_\alpha^2 + \epsilon_\alpha (I_\alpha^2 - \bar{I}_\alpha^2)^{1/2}\cos 2\bar{\theta}_\alpha \quad (\alpha = X,Y). \tag{14}$$

The domain of interest in the phase space for φ_x and $\varphi_{x'}$ is $(0,2\pi)$ and, as one sees from Eq. (11), the corresponding domain for $\bar{\theta}_x$ and for $\bar{\theta}_y$ is $(-\pi,\pi)$. The potential in Eq. (14) is periodic in $\bar{\theta}_\alpha$, with period π. Its maximum occurs at $\bar{\theta}_\alpha = 0$ and $\pm\pi$ and its minimum at $\bar{\theta}_\alpha = \pm\frac{1}{2}\pi$. When the full $(-\pi,\pi)$ domain of $\bar{\theta}_\alpha$ is covered in the motion, the motion is "rotational"; when this domain is not fully explored $\bar{\theta}_\alpha$ oscillates about the point $\bar{\theta}_\alpha = \pi/2$ (or $-\pi/2$).

A separatrix in the $(\bar{I}_\alpha,\bar{\theta}_\alpha)$ phase plane separates the rotational from the oscillatory $\bar{I}_\alpha$ motion. The energy E_α^S for the separatrix found by noting that $\bar{I}_\alpha$ vanishes on the separatrix when $\cos 2\bar{\theta}_\alpha$ reaches its maximum $+1$. Thereby, from Eq. (14), we have

$$E_\alpha^S = \tfrac{1}{2}\epsilon_\alpha I_\alpha. \tag{15}$$

We next consider the conditions for $\bar{I}_\alpha$ to oscillate (i.e., that

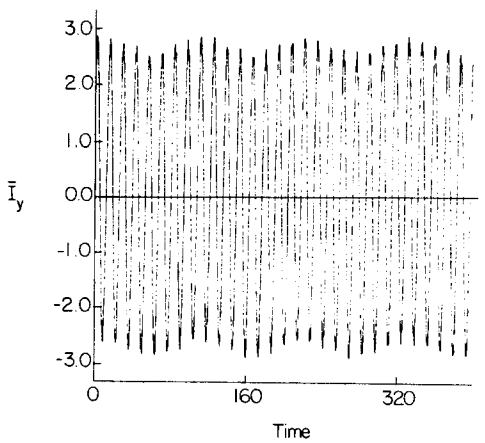

FIG. 10. Oscillating regime near the resonance for $\bar{I}_y$ for the trajectory of Fig. 7.

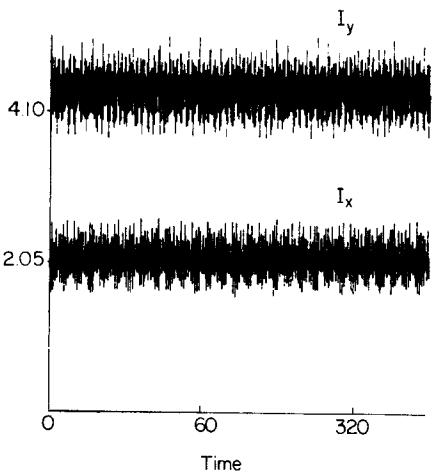

FIG. 12. Approximate invariants of the motion for I_x and I_y modes of the molecule (sixth order), corresponding to the trajectory of Fig. 11.

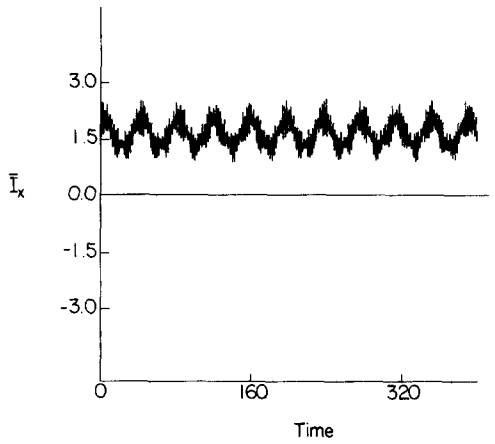

FIG. 13. Rotating regime for $\bar{I}_x$ for the trajectory of Fig. 11.

$E_\alpha < E_\alpha^S$) or rotate ($E_\alpha > E_\alpha^S$), and to understand why the ease in attaining the "rotational" condition differs markedly for $\bar{I}_x$ and $\bar{I}_y$ (cf. Figs. 13 and 14).

We denote the maximum in $\bar{I}_\alpha$ during the motion by $\bar{I}_{\alpha,m}$. Since it occurs at $\cos 2\bar{\theta}_\alpha = -1$, Eq. (14) shows that

$$2E_\alpha = \lambda_\alpha \bar{I}_{\alpha,m}^2 - \epsilon_\alpha (I_\alpha^2 - \bar{I}_{\alpha,m}^2)^{1/2}. \tag{16}$$

In the particular case that the initial value of $J_{\alpha'}$ ($\alpha = X$ or Y) is either small or if, due to energy transfer with $J_\alpha, J_{\alpha'}$ becomes very small at some time during the motion, the maximum value of $\bar{I}_\alpha$ is seen from Eq. (11) to be close to I_α. In this case, Eq. (16) simplifies to

$$E_\alpha \cong \tfrac{1}{2}\lambda_\alpha I_\alpha^2. \tag{17}$$

From Eqs. (15) and (17), one can easily determine the conditions for the $\bar{I}_\alpha$ motion to become localized on the hot ligand (i.e., for the motion of $\bar{I}_\alpha$ to become rotational), namely for $E_\alpha > E_\alpha^S$. Since E_α grows quadratically with I_α, as in Eq. (17), while E_α^S grows only linearly with I_α, as in Eq. (15), the condition $E_\alpha > E_\alpha^S$ is realized when I_α becomes large enough. When λ_α is small, as it is for the $\bar{I}_y$ motion, the condition $E_\alpha > E_\alpha^S$ becomes difficult to attain and so the $\bar{I}_y$ motion remains oscillatory, as in Figs. 10 and 14. From Eqs. (15) and (17), one sees that this condition $E_\alpha > E_\alpha^S$ is attained when I_α exceeds a critical value of I_α^C given by

$$I_\alpha^C = \epsilon_\alpha / \lambda_\alpha. \tag{18}$$

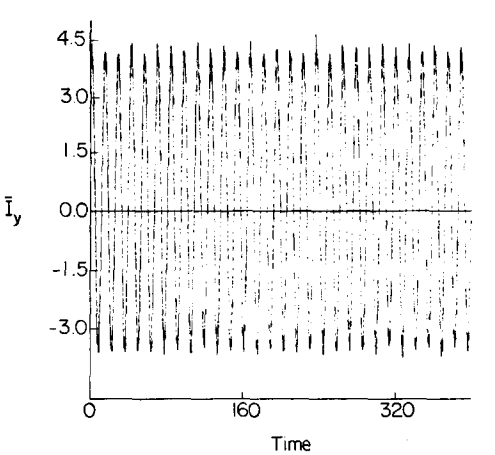

FIG. 14. Oscillating regime resonance for $\bar{I}_y$ for the trajectory of Fig. 11.

For the values of the parameters considered in Sec. II, one finds $\lambda_x = 6.24$, $\epsilon_x = 11.44$, $\lambda_y = 0.99$, and $\epsilon_y = 65.98$, all in units of cm^{-1}. Thereby, $I_x^C \cong 1.83$ and $I_y^C \cong 66.6$. Examining the I_x's and I_y's in Figs. 8 and 12, it becomes clear why in both cases the motion of $\bar{I}_y$ (Figs. 10 and 14) is oscillatory, why it should remain so even at much higher values of I_y, and why the $\bar{I}_x$ motion is oscillatory in Fig. 9 (the I_x in the corresponding Fig. 8 is about 1.5), but rotational in Fig. 13 (I_x in the corresponding Fig. 12 is about 2.1).

Whether or not $\bar{I}_{\alpha,m}$ in Eq. (16) can attain a value nearly equal to I_α during the motion and hence permit use of the very simple Eq. (17), rather than requiring the use of Eq. (16), depends on the initial conditions. If $J_{\alpha'}$ is made relatively small initially, as in the present examples, Eq. (17) becomes an increasingly good approximation to Eq. (16).

From Eq. (14), the frequency of the motion for $\bar{I}_\alpha$ can also be calculated, for any E_α and I_α. Equation (14) can be rearranged to give an equation containing second and zeroth powers of $\bar{I}_\alpha^2$, expressed as a function of powers of $\cos^2 2\bar{\theta}_\alpha$ and E_α. This quadratic equation for the variable $\bar{I}_\alpha^2$ can be solved and the phase integral $\tilde{I}_\alpha$ then calculated:

$$\tilde{I}_\alpha = \oint \bar{I}_\alpha(\bar{\theta}_\alpha, E_\alpha) d\bar{\theta}_\alpha. \tag{19}$$

Here, the domain of $\bar{\theta}_\alpha$ is $(-\pi,\pi)$ for a rotational motion of $\bar{I}_\alpha$ and from turning point to turning point in the case that $\bar{I}_\alpha$ is oscillatory. The frequency $\bar{\omega}_\alpha$ of the $\bar{I}_\alpha$ motion is then calculated from the standard formula

$$\bar{\omega}_\alpha = dE_\alpha / d\tilde{I}_\alpha = (d\tilde{I}_\alpha / dE_\alpha)^{-1}. \tag{20}$$

We omit any further details of $\bar{\omega}_\alpha$, but merely note that a numerical solution of the equations of motion based on the Hamiltonian (13) gave good results for the frequency for the $\bar{I}_y$ motion when there is a frequency gap of $\bar{I}_x$ and $\bar{I}_y$ motions, with or without the λ_{xy} term, at least if the system is not near the separatrix. The $\bar{I}_x$ motion for the conditions in Fig. 13 is a very close to the separatrix and so whether or not it is localized (i.e., rotational) can also be sensitive to the initial conditions. A choice of the initial value of $\bar{I}_x$ very close to I_x produced a rotational motion for the energy for Fig. 10.

We conclude this section by relating the preceding analysis to the matching or near matching of frequencies of the subsystems. The Hamiltonian (14) serves as a "resonance" Hamiltonian for transfer of action between the J_α and $J_{\alpha'}$ modes. It is more complicated than the standard Chirikov Hamiltonian,[9,10] because the amplitude of this cosine term in Eq. (14) can vary markedly from nearly zero to some appreciable value, rather than being a nearly constant. The frequency ω_α of the J_α motion within a ligand is seen from Eq. (10), with the coupling terms λ_{xy}, ϵ_x, and ϵ_y set equal to zero, to be

$$\omega_\alpha = \partial H / \partial J_\alpha = \omega_{0\alpha} - 2\lambda_\alpha J_\alpha. \tag{21}$$

A resonance condition, and hence an extensive transfer of energy between the J_α and $J_{\alpha'}$ modes ($\alpha = X$ or Y), occurs when $\omega_\alpha \cong \omega_{\alpha'}$, i.e., when $J_\alpha \cong J_{\alpha'}$, for similar ligands. If the conditions are such that J_α and $J_{\alpha'}$ are sufficiently different, which may require a high value of $J_\alpha + J_{\alpha'}$ and an initially small $J_{\alpha'}$, ω_α and $\omega_{\alpha'}$ can be sufficiently different that a localization of the energy in the J_α mode can be achieved. We

have seen that this condition is difficult to achieve for the Y and Y' modes (i.e., for the $\bar{I}_y$ motion)—there is too easy an energy transfer between the L–M and M–R modes—but it is achievable for the X and X' modes. Thereby, the restriction to the energy transfer is concentrated primarily in the intraligand modes J_x and $J_{x'}$.

IV. DISCUSSION

From the results of Secs. II and III, the following profile of the response of the system to increasing the excitation energy can be given: The local group modes involve collective motions of the ligands of the heavy central mass. A low-frequency mode in each ligand (the Y mode) has as its motion primarily that of the center of mass of a ligand vs the heavy atom; a high-frequency mode (the X mode) can be viewed as a relative motion of atoms within this ligand. Two key couplings occur in the local mode interaction: that between the modes of a particular ligand–metal atom subsystem, and that leading to the resonances between modes of the two subsystems. The rate and extent of energy transfer results from the interplay of both mechanisms. The former governs energy exchange within one ligand, while the latter regulates its flow between ligands.

At least for a moderate degree of excitation, the $\bar{I}_x$ and $\bar{I}_y$ motions appear to be approximately separable. Simultaneously, the ligand–ligand interaction may be explained as a 1:1 resonance between equivalent modes (J_x with $J_{x'}$ and J_y with $J_{y'}$). For very low excitations, namely for E_1 less than 0.1 D, the $\bar{I}_x$ and $\bar{I}_y$ motions are both oscillatory. The motion of the system is indeed expected to be largely that of somewhat perturbed normal modes of the whole chain. As the initial excitation energy is increased slightly, both the $\bar{I}_x$ and the $\bar{I}_y$ motion continue to be oscillatory, with the $\bar{I}_y$ motion having the higher frequency of oscillation for the ligand to ligand energy transfer. There is no barrier to the energy flow in this region. Ultimately, the relatively small energy needed to exceed that of the separatrix of the resonance in the $\bar{I}_x$ motion is responsible for the energy localization. Because of this small critical energy, the $\bar{I}_x$ motion changes, for higher excitation, rapidly from oscillation about the resonance center to rotation, while the $\bar{I}_y$ motion is still quasiharmonically oscillating. That is, the former, a primarily asymmetric ligand–ligand motion, serves to localize the energy while the other, a primarily asymmetric ligand–M–ligand motion, still transfers it.

The 1:1 resonance approximation used in Sec. II ceases to be valid when, at higher excitations, other X mode resonances become accessible to the system. These resonances arise from the neglected terms in the double Fourier expansion of the coupling term V_{LR} in Eq. (9). As is well known, the presence of several accessible resonances leads to an irregular ("chaotic") motion whenever the resonances begin to "overlap" (Chirikov theory), and power spectra then become grassy. With this aspect in mind we next consider the behavior in Figs. 3 and 4. A detailed analysis of this trajectory is beyond the scope of the present paper, which focuses instead on an analysis of the clearly quasiperiodic regime of $E_1 < 0.4$ D. However, a few remarks are in order. The most striking feature in Fig. 4 ($E_1 = 0.5$ D) is that the low frequency peaks remain sharp while the high frequency ones and the combination band have become grassy. It follows that the approximate separation of the (X,X') motions from the (Y,Y') ones found at $E_1 < 0.4$ D continues at $E_1 = 0.5$ D. The sharp low frequency lines show that the motion of I_y and $\bar{I}_y$ continues to be quasiperiodic. The grassy appearance of the other bands cannot be due to $\bar{I}_x$ moving outside a resonance: A comparison of Fig. 9 with Fig. 13 shows that it already did so at an $E_1 = 0.15$ D and indeed such a move is expected to simplify the spectra. It could, of course, be due to $\bar{I}_x$ moving into a new isolated resonance. Then to explain the grassy behavior in Fig. 4 one would presumably need to postulate that r_1 and r_4 are complicated functions of I_y,$\bar{I}_y$ and of the (X,X') variables at $E_1 = 0.5$ D. (An isolated resonance yields a simple spectrum, a set of equally spaced lines in a single coordinate case, and hence the need to invoke complicated functions for r_1 and for r_4, yielding many Fourier components.) Alternatively, the grassy appearance could be due to the onset of chaotic behavior[12] in the (X,X') motion. Indeed, the inability to back integrate this trajectory in double precision provides some evidence for this possibility. We shall not attempt to resolve this interesting question in the present paper.

Noting the above behavior of reducing to two separate two-coordinate problems for this five-atom system, one involving the X and X' motion and the other the Y and Y' motion, we briefly consider the induction period observed in Fig. 3. This induction period has been presumed in systems of two (chaotic) degrees of freedom to be related to the mean time[13] needed to exit an area of phase space confined by the remnants of an invariant torus.[14–16] Such a confinement need not occur in systems having a higher number of coupled anharmonic degrees of freedom.

At very high values of E_1 ($= 0.7$ D) a second clearly quasiperiodic regime for the entire system enters. We have not studied and attempted to characterize it as yet.

The $\bar{I}_y$ motion was seen earlier to occur deep in a potential well, in virtue of the small value of λ_y and the large value for ϵ_y, for the given I_y. The $\bar{I}_x$ motion was seen to be closer to the separatrix. Perhaps for this reason the $\bar{I}_y$ motion appears to remain quasiperiodic in Figs. 3 and 4, while the $\bar{I}_x$ motion showed a greater tendency to have a more complicated power spectrum (Fig. 4).

Using the above results, we next consider the behavior which might be predicted for system with many coordinates, i.e., for systems which approximate real molecules more closely. The Y and Y' modes were primarily the low frequency L vs M and M vs R motions, and are expected to remain so when L and R each become larger than a mere CC bond. For the conditions studied for Figs. 10 and 14, there was an easy energy exchange between these L vs M and M vs R modes. However, in large molecules this energy becomes typically only a small fraction of the total. The X and X' modes were primarily CC vibrations and now become primarily vibrations within L and R, respectively. At moderate energies they ceased to exchange energy significantly, but at energies where the power spectra became grassy they did so, *though only after an induction period*. A similar behavior can occur for the larger molecular system under certain conditions.

One condition for this energy localization in the excited ligand in larger systems is that there continue to be an approximate separation of the (X,X') from the (Y,Y') variables. In the present case, the frequency of the L vs M (and M vs R) motion was substantially less than that of the modes within L and R. Larger ligands will have some low frequency modes. If they are not coupled to the (Y,Y') variables, the approximate separation of variables can again occur. It is interesting to note therefore that in Ref. 2, which gave numerical results for larger systems, there was little energy transfer at moderate energies.

In the present analysis, attention has been focused for simplicity on the kinetic coupling in the C–M–C stretching motions. Potential energy coupling and a bending C–M–C coupling can also occur. This bond angle motion does not, however, appear to be involved in any major low order resonance (e.g., 1:1 or 1:2) with the C–M–C stretches, for the real molecules that we have examined. The results of Ref. 2, which included both of these additional couplings are thereby of added interest.

Perhaps the most striking finding in the present analysis is the approximate separation of variables in the primarily intraligand–intraligand motion from those in the primarily ligand–metal–ligand motion, a separation which appears in the clearly quasiperiodic regime for $E_1 \leqslant 0.4$ D and in the new regime ($E_1 \sim 0.5$ D) whose power spectrum is grassy for certain lines and sharp for others.

The present calculations are classical. Some quantum mechanical calculations have been made in our group on the present system.[17] We found that energy transfer occurs even when little occurred classically and hence that it occurred in that case by a tunneling mechanism and, thereby, at a reduced rate. Evidence is also obtained again for the approximate separation of variables. A detailed description of the results will be presented elsewhere.

ACKNOWLEDGMENTS

It is a pleasure to acknowledge the support of the National Science Foundation and of the U.S.–Spain Committee for Scientific and Technological Cooperation. We also acknowledge fruitful discussions with Dr. V. K. Babamov and invaluable computational assistance from Dr. D. W. Noid.

APPENDIX A: PERTURBATION HAMILTONIAN FOR METAL–LIGAND SUBSYSTEM

A perturbation technique is used in this appendix to find the approximate constants of the motion for H_L, and for H_R, and to examine the transition from nonlocalizing to localizing group mode trajectories at excitation energies $E_1 < 0.4$ D. For this range of energies, the vibrational modes in H_L and H_R cannot be too different from normal modes. Therefore, a perturbation scheme is used, the reference Hamiltonian being the one for which normal modes are valid. The Morse potentials are first expanded in a Taylor series around the equilibrium position

$$\sum_{i=1}^{2} D(1-e^{-a(r_i-r_i^e)})^2 = 2D\sum_{n=2}^{\infty}(-1)^n\frac{(2^{n-1}-1)}{n!}a^n \times[(r_1-r_1^e)^n+(r_2-r_2^e)^n]. \tag{A1}$$

The Hamiltonian H_L is then divided into two parts

$$H_L = H_0 + V, \tag{A2}$$

where H_0 contains the quadratic terms

$$H_0 = \tfrac{1}{2}g_{11}p_1^2 + \tfrac{1}{2}g_{22}p_2^2 + g_{12}p_1p_2 + Da^2[(r_1-r_1^e)^2+(r_2-r_2^e)^2] \tag{A3}$$

and V the anharmonic corrections

$$V = \sum_{n=3}^{\infty} 2Da^nV^{(n)},$$

where

$$V^{(n)} = \frac{(-1)^n(2^{n-1}-1)}{n!}[(r_1-r_1^e)^n+(r_2-r_2^e)^n]. \tag{A4}$$

H_0 is an integrable Hamiltonian of a system that can be written as the sum of two independent harmonic oscillators of unit mass

$$H_0 = \tfrac{1}{2}(p_x^2+p_y^2+\omega_{0x}^2x^2+\omega_{0y}^2y^2). \tag{A5}$$

where x and y are normal mode coordinates obtained from r_1 and r_2 by a linear transformation. In this notation x represents the high frequency normal mode and $so\omega_{0x} > \omega_{0y}$.

The anharmonic correction V has the following form in these new coordinates:

$$V = \sum_{n=3}^{\infty}\sum_{i+j=n}^{\infty} B_{ij}x^iy^j, \tag{A6}$$

where the B_{ij} are combinations[18] of the g_{11}, g_{12}, and g_{22} appearing in Eq. (A3).

There is, therefore, a classical nonintegrable Hamiltonian

$$H = \tfrac{1}{2}(p_x^2+\omega_{0x}^2x^2)+\tfrac{1}{2}(p_y^2+\omega_{0y}^2y^2)+\sum_{n=3}^{\infty}\sum_{i+j=n} B_{ij}x^iy^j \tag{A7}$$

which for low energies can be approximated with a few terms and in which the nonintegrable part is a homogeneous polynomial in the coordinates.

An appropriate procedure for this case that permits the transformation of this Hamiltonian into a normal form, consisting of a power series of one dimensional uncoupled harmonic oscillators, has been given by Birkhoff[19] and modified by Gustavson[20] to include systems with commensurable frequencies. This procedure has been reviewed elsewhere.[21]

The Birkhoff–Gustavson method was implemented with the aid of an automatic algebraic manipulator (SMP)[22] to obtain H_L (H_R) in the normal form

$$H_L = \sum_n H^{(n)} = \sum_n\sum_{r+s=n} C_{rs}^{(n)}[P_x^{(n)^2}+X^{(n)^2}]^r \times[P_y^{(n)^2}+Y^{(n)^2}]^s. \tag{A8}$$

This result can be achieved by successive canonical transfor-

TABLE I. Coefficients of the sixth order normal form of H_L (H_R).[a]

C_{10}	1014.244 245	C_{20}	−6.235 703 968	C_{03}	−0.004 006 13
C_{01}	420.166 950 6	C_{02}	−0.985 135 279 6	C_{21}	−0.049 362 9
C_{11}	−4.567 716 084	C_{30}	0.004 999 26	C_{12}	0.038 390 3

[a] Units of the C_{ij}'s are cm^{-1}.

mations of the so called F_2 type, $F_2^{(m)}$ being the mth generating function:

$$F_2^{(m)} = P_x^{(m)} X^{(m-1)} + P_y^{(m)} Y^{(m-1)} + W(P_x^{(m)}, P_y^{(m)}, X^{(m-1)}, Y^{(m-1)}), \quad \text{(A9)}$$

where $P_x^{(m)}$ and $P_y^{(m)}$ are a new momenta and $X^{(m-1)}$ and $Y^{(m-1)}$ are the old coordinates. The transformations equations are

$$X^{(m)} = X^{(m-1)} + \frac{\partial W^{(m)}}{\partial P_x^{(m)}}, \quad Y^{(m)} = Y^{(m-1)} + \frac{\partial W^{(m)}}{\partial P_y^{(m)}},$$

$$P_x^{(m-1)} = P_x^{(m)} + \frac{\partial W^{(m)}}{\partial X^{(m-1)}},$$

$$P_y^{(m-1)} = P_y^{(m)} + \frac{\partial W^{(m)}}{\partial Y^{(m-1)}}, \quad \text{(A10)}$$

where $X^{(m)}$ and $Y^{(m)}$ are new coordinates and $P_x^{(m-1)}$ and $P_y^{(m-1)}$ are the old momenta.

The generating function $W^{(m)}$ was obtained analytically up to and including $m = 4$. The normal form of H_L including terms up to $H^{(5)}$ is given by Eq. (A11) (the odd order terms vanish)

$$H_L = \omega_{0x} J_x + \omega_{0x} J_y - \lambda_x J_x^2 - \lambda_y J_y^2 - \lambda_{xy} J_x J_y, \quad \text{(A11)}$$

where

$$\lambda_x = -\frac{3}{2} b_{40} + \frac{15 b_{30}^2}{4\omega_{0x}} + \frac{b_{21}^2 (8\omega_{0x}^2 - 3\omega_{0y}^2)}{4\omega_{0y}(4\omega_{0x}^2 - \omega_{0y}^2)},$$

$$\lambda_y = -\frac{3}{2} b_{04} + \frac{15 b_{03}^2}{4\omega_{0y}} + \frac{b_{12}^2 (8\omega_{0y}^2 - 3\omega_{0x}^2)}{4\omega_{0x}(4\omega_{0y}^2 - \omega_{0x}^2)},$$

$$\lambda_{xy} = -b_{22} + \frac{3 b_{03} b_{21}}{\omega_{0y}} + \frac{3 b_{30} b_{12}}{\omega_{0x}} - \frac{2\omega_{0y} b_{12}^2}{(\omega_{0x}^2 - 4\omega_{0y}^2)} - \frac{2\omega_{0x} b_{21}^2}{(\omega_{0y}^2 - 4\omega_{0x}^2)}. \quad \text{(A12)}$$

The b_{ij}'s are related to the coefficients appearing in Eq. (A7), $b_{ij} = B_{ij}/(\omega_{0x}^i \omega_{0y}^j)^{1/2}$, and J_x and J_y in Eq. (A11) are the standard harmonic oscillator actions for the fourth order variables X, P_x, Y, and P_y.

These transformations have also been performed up to sixth order when the numerical values of the model system under study are used for ω_{0x}, ω_{0y}, and b_{ij}. The C_{ij}'s in the resulting Hamiltonian

$$H_L = \sum_{ij=0}^{3} C_{ij}^{(6)} J_x^{(6)i} J_y^{(6)j} \quad \text{(A13)}$$

are given in Table I for all (i,j) pairs whose sum lies between 1 and 3.

This approximate Hamiltonian is well suited[23] for EBK semiclassical quantization, and the accuracy of Eq. (A13) has been tested, by comparing the EBK semiclassical eigenvalues E_i^{SC} obtained from Eqs. (A11) and (A13) with the quantum eigenvalues E_i^Q obtained with a variational calculation using Morse wave functions as the basis set. In Table II we present numerical values of $E_i^Q - E_0^Q$ and of the $E_i^{SC} - E_0^{SC}$ obtained[24] with Eqs. (A11) and (A13) for $i \leqslant 30$, together with the number of quanta n_x and n_y in the X and Y modes, respectively. For eigenvalues with less than ten quanta in any mode, the quantity $E_i^{SC} - E_0^{SC}$ reproduces $E_i^Q - E_0^Q$ within 0.1%. Therefore, it can be expected that the actions $J_x^{(6)}$ and $J_y^{(6)}$ for the sixth order calculation represent with some accuracy the constants of the H_L motion for the range of energy containing at least up to the 30 quantum states in Table II. Thus, for sufficiently low energy, the motion of the C–C–Sn model system almost lies on the sur-

TABLE II. Comparison of variational eigenvalues E_i^Q of H_L and semiclassical values E_i^{SC} obtained with Eq. (A11).[a]

n_x	n_y	$E_i^Q - E_0^Q$ (cm^{-1})	$E_i^{SC(4)} - E_0^{SC(4)}$ (cm^{-1})	$E_i^{SC(6)} - E_0^{SC(6)}$ (cm^{-1})
0	1	415.913	415.913	415.925
0	2	829.859	829.855	829.884
1	0	999.482	999.489	999.465
0	3	1241.81	1241.83	1241.85
1	1	1410.80	1410.83	1410.80
0	4	1651.75	1651.83	1651.80
1	2	1820.24	1820.21	1820.25
2	0	1986.49	1986.51	1986.45
0	5	2059.64	2059.86	2059.71
1	3	2227.76	2227.61	2227.78
2	1	2393.12	2393.28	2393.10
0	6	2465.46	2465.92	2465.55
1	4	2633.35	2633.05	2633.37
2	2	2797.92	2798.09	2797.94
0	7	2869.18	2870.01	2869.31
3	0	2961.05	2961.05	2961.00
1	5	3036.99	3036.51	3036.99
2	3	3200.90	3200.93	3200.93
0	8	3270.76	3272.13	3270.96
3	1	3362.88	3363.26	3362.86
1	6	3438.66	3438.00	3438.73
2	4	3602.03	3601.79	3602.06
0	9	3670.19	3672.29	3670.47
3	2	3762.96	3763.50	3762.98
1	7	3838.32	3837.53	3838.26
4	0	3923.22	3923.13	3923.13
2	5	4001.28	4000.69	4001.31
0	10	4067.42	4070.47	4067.82
3	3	4161.27	4161.67	4161.34
1	8	4235.96	4235.08	4235.86

[a] n_x and n_y are the number of quanta in the X and Y modes. $E_i^{SC(4)}$ and $E_i^{SC(6)}$ are obtained to fourth order [Eq. (A11)] and sixth order, respectively. $E_0^Q = 715.084$ cm^{-1}, $E_0^{SC(4)} = 714.258$ cm^{-1}, $E_0^{SC(6)} = 714.257$ cm^{-1}.

face of an invariant torus of radii given by $J_x^{(6)}$ and $J_y^{(6)}$. The $X^{(6)}$ motion in this torus mainly corresponds to the vibration of the C–C bond with a frequency $\partial H_L/\partial J_x^{(6)}$ or, using Eq. (A13),

$$\omega_x = \sum_{ij=0}^{3} iC_{ij}^{(6)} J_x^{(6)i-1} J_y^{(6)j}, \tag{A14}$$

whereas the $Y^{(6)}$ motion corresponds mostly to the vibration of the C–C center of mass against the Sn, with a lower frequency

$$\omega_y = \sum_{ij=0}^{3} jC_{ij}^{(6)} J_x^{(6)i} J_y^{(6)j-1}. \tag{A15}$$

Comparison of the numerical values of these frequencies using the $C_{ij}^{(6)}$'s given in Table I shows the difference in anharmonicities between the two group modes. The X mode, with higher frequency, has also a larger anharmonicity ($C_{20} \cong 6.3\, C_{02}$).

[1] V. Lopez and R. A. Marcus, Chem. Phys. Lett. **93**, 232 (1982). The masses used there and in the present paper 22 063.6065 and 218 027.596 a.u. are within a percent of the masses of C and Sn. In a.u., the D, a, and r_i^e used in Eq. (1) are exactly 0.134, 0.815, and 2.91, respectively.

[2] K. N. Swamy and W. H. Hase, J. Chem. Phys. **82**, 123 (1985).

[3] E. B. Wilson, J. C. Decius and P. C. Cross, *Molecular Vibrations* (McGraw-Hill, New York, 1955).

[4] C. C. Rankin and W. H. Miller, J. Chem. Phys. **55**, 3150 (1971). This action variable is (in units of $\hbar = 1$) the classical equivalent of $n + 1/2$, where n is a continuous variable classically and an integer quantum mechanically. It is canonically conjugate to an angle variable which varies over an interval of 2π. The conventional action variable is instead $(n + 1/2)h$ or, in units of $\hbar = 1$, $2\pi(n + 1/2)$ and is conjugate to an angle variable which varies over a unit interval.

[5] M. K. Gordon, Sandia Laboratories Report, SAND 75-0211; L. F. Shampine and M. K. Gordon, *Computer Solution of Ordinary Differential Equations* (Freeman, San Francisco, 1975). We are particularly indebted to Dr. D. W. Noid of Oak Ridge National Laboratory for obtaining the quadruple-precision trajectories.

[6] C. Jaffé and P. Brumer, J. Chem. Phys. **73**, 5646 (1980); C. Jaffé, *ibid.* **81**, 616 (1984).

[7] E. L. Sibert III, W. P. Reinhardt, and J. T. Hynes, J. Chem. Phys. **77**, 3583 (1982); R. M. Hedges and W. P. Reinhardt, *ibid.* **78**, 3964 (1983); S. K. Gray and M. S. Child, Mol. Phys. **53**, 961 (1984).

[8] The adiabatic separation between the slower motion along the Sn–CC coordinate and the faster motion along the C–C coordinate is analogous to the separation of the F–HH and the H–H motion in the collinear F–H–H system, first discussed by V. K. Babamov and A. Kuppermann [J. Chem. Phys. **77**, 189 (1982)]. The latter is believed there to be responsible for the stability of the long lived states (resonances) in the collinear $F + H_2$ collision.

[9] B. V. Chirikov, Phys. Rep. **52**, 263 (1979).

[10] A. J. Lichtenberg and M. A. Lieberman, *Regular and Stochastic Motion* (Springer, New York, 1983).

[11] From Hamilton equations for the two independent oscillators of Hamiltonian (3a), it is easy to obtain frequencies ω_{0x} and ω_{0y} as those of the linearized motion around the minima of their potentials. From the coefficients of the linear transformation from local to normal mode momenta $P_2 = -a_x p_x + a_y p_y$, we get $\epsilon_x = \omega_{0x} a_x^2/M$, $\epsilon_y = \omega_{0y} a_y^2/M$, with M as the mass of the central atom.

[12] D. W. Noid, M. L. Koszykowski, and R. A. Marcus, J. Chem. Phys. **67**, 404 (1977).

[13] I. C. Percival, AIP Conf. Proc. No. 57, 302 (1979); R. S. MacKay, J. D. Meiss, and I. C. Percival, Physica D **13**, 55 (1984).

[14] S. Aubry, in *Solutions and Condensed Matter Physics*, edited by A. R. Bishop and T. Schneider (Springer, Berlin, 1978), p. 264.

[15] J. N. Mather, Topology, **21**, 457 (1982); A. Katok, Ergodic Theory Dynam. Sys. **2**, 185 (1982).

[16] R. B. Shirts and W. P. Reinhardt, J. Chem. Phys. **77**, 5204 (1982).

[17] S. M. Lederman, V. Lopez, G. A. Voth, and R. A. Marcus, Chem. Phys. Lett. **124**, 93 (1986).

[18] The B_{ij}'s are the coefficients obtained upon substitution of the linear transformation from local to normal coordinates in Eq. (A6).

[19] G. D. Birkhoff, *Dynamical Systems* (American Mathematical Society, New York, 1966).

[20] F. G. Gustavson, Astron. J. **71**, 670 (1966).

[21] E.g., T. Uzer, D. W. Noid, and R. A. Marcus, J. Chem. Phys. **79**, 4412 (1983), see Appendix A.

[22] SMP in a symbolic manipulation program developed by the High Energy Physics group at Caltech.

[23] R. T. Swimm and J. B. Delos, J. Chem. Phys. **71**, 1706 (1979).

[24] The numerical values of $\lambda_x, \lambda_y, \lambda_{xy}$ equal the $-C_{20}$, $-C_{02}$, and $-C_{11}$ given in Table I and $C_{10} = \omega_{0x}$, $C_{01} = \omega_{0y}$.